IMPLICIT SURFACE SEGMENTATION BY MINIMAL PATHS, APPLICATIONS IN 3D MEDICAL IMAGES

Roberto Ardon and Laurent D. Cohen

CEREMADE, Université Paris Dauphine, France

roberto.ardon@centraliens.net, cohen@ceremade.dauphine.fr

Anthony Yezzi

Georgia Institute of Technology, USA

ayezzi@ece.gatech.edu

ABSTRACT

In this paper we introduce a novel edge-based, implicit approach for single object segmentation in 3D images. From a couple of curves, traced by the user on the object to be segmented, we implicitly generate a surface that contains the set of minimal paths joining them. These paths are minimal with respect to a cost function that takes lower values on the object to be extracted, hence they are within a small distance from it. Unlike other variational approaches, our method is not concerned with local minima traps. Our algorithm has been successfully applied to 3D medical images and synthetic images.

1. INTRODUCTION

Since their introduction by Kass et al. [1], deformable models have been extensively used to find single and multiple objects in 2D and 3D images. The common use of these models consists in introducing an initial object in the image and transforming it until it reaches a wanted target. In most applications, the evolution of the object is done in order to minimize an energy attached to the image data, until a steady state is reached. One of the main drawbacks of this approach is that it suffers from local minima 'traps'. This happens when the steady state, reached by the active object, does not correspond to the target but to another local minimum of the energy. Thus, the active object initialization is a fundamental step. Since the publication of [1], much work has been done in order to free active models from the problem of local minima. A balloon force was early proposed in [2] to make the model more active and to cope with the shrinking problem, but this force supposed a known direction in the evolution. The introduction of region dependent energies [3, 4] and the use of shape priors approaches [5], contributed to create a more robust framework. In this work, we focus on a novel approach for 3D single object segmentation having a cylinder-like topology. Our contribution consists in implicitly generating a surface

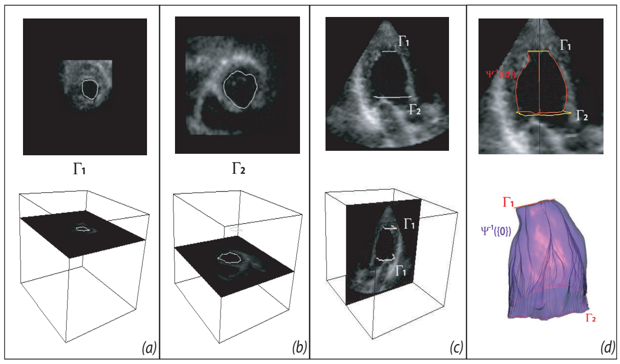

Figure 1: 3D ultrasound volume of a left ventricle: (a) and (b) show the two parallel slices where the user given curves Γ_1 and Γ_2 are drawn. (c) shows a perpendicular slice to the curves in order to show their position with respect to the ventricle. (d) shows the obtained surface containing the constraint curves.

that segments the object between two curves (Γ_1 and Γ_2) introduced in the image by the user and which are the initialization of our model. This surface is obtained as the zero level set of the solution of a linear partial differential equation. Extending the method introduced in [6], the surface we generate contains all globally minimal paths (in a sense we shall further specify) between Γ_1 and Γ_2 and thus is not concerned with local minma traps. As an illustration of the situation we are working on, we give in figure 1 an example of the user input to our algorithm for the segmentation of a 3D ultrasound volume of the left ventricle.
We begin in section 2 by recalling the principles of geodesic active contours as well as the global minimal paths framework. Section 3 exposes our contribution and in section 4 we show some results.

2. MINIMAL PATHS IN 2D IMAGES

2.1. Active contour model

The first active contour model was introduced by Kass *et al.* in the seminal paper [1]. Their model, the well known

This work was supported by MEDISYS-Philips France, 51 rue Carnot 92156 Suresnes, France

0-7803-9134-9/05/$20.00 ©2005 IEEE

'snakes', consists in finding a curve $\mathcal{C}$ (parametrized on an interval J and traced on the image) that minimizes :

$$E_{snake}(\mathcal{C})=\int_J \alpha \|C'(x)\|^2 + \beta \|C''(x)\|^2 + \mathcal{P}(\mathcal{C}(x))dx, \quad (1)$$

where α and β are positive constants. The potential function $\mathcal{P}$ usually represents an edge detector that has lower values on edges. A common choice of this function is $\mathcal{P} = (1 + |\nabla I|^2)^{-1}$, if I is the image. Finding a curve that minimizes energy E is not a simple task; this functional is defined on the infinitely dimensioned space of regular curves and, generally, it is non-convex. The usual approach is based on finding a local minimum of E_{snake} by evolving an initial curve $\mathcal{C}_0$ under the time dependent equation $\frac{\partial \mathcal{C}(x,t)}{\partial t} - \alpha \frac{\partial^2 \mathcal{C}(x,t)}{\partial x^2} + \beta \frac{\partial^4 \mathcal{C}(x,t)}{\partial x^4} = -\nabla \mathcal{P}(\mathcal{C})$, with $\mathcal{C}(\cdot, 0) = \mathcal{C}_0$ until convergence. By construction, the final curve $\mathcal{C}$ is strongly dependent on the initialization $\mathcal{C}_0$. Since the method was originally intended to segment a single object in the image, this behavior is rather natural. Nonetheless, if $\mathcal{C}_0$ is too far from the object to extract, the evolving curve can be trapped by a different, unsatisfactory, local minimum.

2.2. Active contours and minimal paths

In order to obtain global minimization in the active contours framework, Cohen and Kimmel [6] simplified the energy by choosing $\beta = 0$ in the expression (1) of E. Additionally, they propose to use arclength parameterization (here noted s). Thus, they look for the curve minimizing the energy $E(\mathcal{C}) = \int_0^L \{\alpha + \mathcal{P}(\mathcal{C}(s))\} ds$, where L is the length of curve $\mathcal{C}$ (in the rest of this paper we shall note $\widetilde{\mathcal{P}} = \alpha + \mathcal{P}$). Even though this is the same energy proposed by Caselles *et al* in [7], used in the well-known geodesic active contour model, Cohen and Kimmel choose a completely different approach for the minimization of E. Instead of using an evolution equation as in [1] and [7], they exploit a method capable of building a curve between two points (p_1 and p_2) which is the global minimum of E among all the curves joining these points. This minimum is called a minimal path. Moreover, these authors obtain this minimal path by following the opposite gradient direction on the minimal action map, defined in each point q by :

$$U_{p_1}(q) = \inf_{\substack{\text{all curves such that} \\ \mathcal{C}(0)=p_1, \mathcal{C}(L)=q}} \left\{ \int_0^L \widetilde{\mathcal{P}}\big(C(s)\big) ds \right\}. \quad (2)$$

The minimal path between p_2 and p_1 is thus obtained by solving the problem:

$$\frac{d\mathcal{C}}{dx}(x) = -\nabla U_{p_1}\big(\mathcal{C}(x)\big) \text{ with } \mathcal{C}(0) = p_2. \quad (3)$$

In order to compute U_{p_1}, Cohen and Kimmel [6] use the fact (a proof can be found in [8]) that this map is solution to the well known Eikonal equation : $\|\nabla U_{p_1}\| = \widetilde{\mathcal{P}}$ and $U_{p_1}(p_1) = 0$. Equation (3) can be numerically solved by ordinary differential equations techniques like Newton 's or Runge-Kutta's. To numerically solve the Eikonal equation, classic finite differences schemes tend to be unstable. In [9] Tsitsiklis introduced a new method that was independently reformulated by Sethian [10]. It relies on a one-sided derivative looking in the direction of the information flow, and it gives a consistent approximation of the weak solution to the Eikonal equation. This algorithm is known as the Fast Marching algorithm and is now widely used and understood. It was used in [6] for the computation of minimal paths. This algorithm has an $O(N \log(N))$ complexity on a grid of N nodes, and only one grid pass is needed to give a first order approximation of the solution U_{p_1}.

3. FROM GLOBAL MINIMAL PATHS TO 3D SURFACE EXTRACTION

The method introduced in [6] can easily be extended for the construction of minimal paths between two points in a 3D image [11]. In that case, the formalism given in the previous section is unchanged, except from the fact that functions $\widetilde{\mathcal{P}}, U_{p_1}$ are defined (and $\mathcal{C}$ takes its values) on a 3D domain. As in the previous section, the cost function $\widetilde{\mathcal{P}}$ is supposed to have lower values on a surface to extract from the 3D image. Following [12], we further extend the minimal path framework to the extraction of this surface between two given curves Γ_1 and Γ_2. We exploit the idea of building a set of minimal paths between these curves. The main contribution of our work consists in introducing an implicit approach that outputs a real function Ψ, defined on the image domain, such that its zero level set surface contains the set of minimal paths. This avoids to get holes in the surface due to the fact that minimal paths may turn around a bump region. Also, interpolation is not needed anymore.

3.1. Minimal path set $\mathcal{S}_{\Gamma_1}^{\Gamma_2}$

We shall say that $\mathcal{C}$ is a path between a point q and a curve Γ_1 if $\mathcal{C}(0) = q$ and $\mathcal{C}(L) \in \Gamma_1$. Similarly to section 2.2, the minimal path between Γ_1 and a point q (further noted $\mathcal{C}_{\Gamma_1}^q$) can be obtained by performing a gradient descent on the action map U_{Γ_1}, which is defined on each point by :

$$U_{\Gamma_1}(q) = \inf_{\substack{\text{all curves such that} \\ \mathcal{C}(0)=q, \mathcal{C}(L)\in\Gamma_1}} \left\{ \int_0^L \widetilde{\mathcal{P}}(\mathcal{C}(s)) ds \right\}. \quad (4)$$

$\mathcal{C}_{\Gamma_1}^q$ satisfies for all x of its interval of definition:

$$\frac{d\mathcal{C}_{\Gamma_1}^q}{dx}(x) = -\nabla U_{\Gamma_1} \; \mathcal{C}_{\Gamma_1}^q(x) \quad \text{with } \mathcal{C}_{\Gamma_1}^q(0) = q. \quad (5)$$

Furthermore, notice that $U_{\Gamma_1}(q) = \inf_{p\in\Gamma_1} \{U_p(q)\}$, where U_p is the action map associated to point p as defined in section 2.2 by equation (2). This implies that a first order numerical estimation of U_{Γ_1} can also be obtained through the Fast marching algorithm, initializing U_{Γ_1} by $U_{\Gamma_1}(q) = 0$ if $q \in \Gamma_1$ and $U_{\Gamma_1}(q) = \infty$ otherwise.
Consider the set $\mathcal{S}_{\Gamma_1}^{\Gamma_2}$ of minimal paths $\left\{\mathcal{C}_{\Gamma_1}^q\right\}_{q\in\Gamma_2}$ between curve Γ_1 and each point q of the curve Γ_2. As in [12], we make the hypothesis that each path of $\mathcal{S}_{\Gamma_1}^{\Gamma_2}$, if not traced on the surface to extract, is within a small distance from it.

3.2. Implicit generation of a surface containing $\mathcal{S}_{\Gamma_1}^{\Gamma_2}$

In this section, we suppose that Γ_1 and Γ_2 are two non-intersecting planar and closed curves. Following the idea of the Level Set method introduced by Osher and Sethian [13], we look for a real function Ψ, defined on the image domain Ω, such that $\mathcal{S}_{\Gamma_1}^{\Gamma_2}$ is contained in its zero level set (further noted $\Psi^{-1}(0)$).
Necessary condition : Let us first suppose the existence of such a function, that is $\mathcal{S}_{\Gamma_1}^{\Gamma_2} \subset \Psi^{-1}(0)$. Consider a minimal path of $\mathcal{S}_{\Gamma_1}^{\Gamma_2}$, $\mathcal{C}_{\Gamma_1}^q$, parameterized on an interval J. Supposing that Ψ is differentiable, we obtain, from the derivation with respect to x of the relation $\Psi(\mathcal{C}_{\Gamma_1}^q(x)) = 0$, that $\forall x \in J$, $\nabla\Psi(\mathcal{C}_{\Gamma_1}^q(x)).\frac{d\mathcal{C}_{\Gamma_1}^q}{dx}(x) = 0$. Then, using (5) we obtain that for all p of a path of $\mathcal{S}_{\Gamma_1}^{\Gamma_2}$:

$$\nabla\Psi(p).\nabla U_{\Gamma_1}(p) = 0. \tag{6}$$

Sufficient condition : Conversely, let Ψ be a real differential function defined in Ω and satisfying for all point $p \in \Omega$ relation (6).
If $\forall q \in \Gamma_2$, $\Psi(q) = 0$, then we have $\mathcal{S}_{\Gamma_1}^{\Gamma_2} \subset \Psi^{-1}(0)$.
Indeed, for all point $q \in \Gamma_2$, the derivation of the function $f_q : x \longrightarrow \Psi \circ \mathcal{C}_{\Gamma_1}^q(x)$, gives:

$$\begin{array}{rcl} \frac{df_q}{dx}(x) & = & \nabla\Psi\ \mathcal{C}_{\Gamma_1}^q(x)\ .\frac{d\mathcal{C}_{\Gamma_1}^q}{dx}(x) \\ & = & -\nabla\Psi\ \mathcal{C}_{\Gamma_1}^q(x)\ .\nabla U_{\Gamma_1}\ \mathcal{C}_{\Gamma_1}^q(x) \quad = \quad 0. \end{array}$$

Thus, for each $q \in \Gamma_2$, function f_q is constant. Furthermore, since $f_q(0) = \Psi \circ \mathcal{C}_{\Gamma_1}^q(0) = \Psi(q) = 0$, we finally have $\forall q \in \Gamma_2, \forall x, \Psi\big(\mathcal{C}_{\Gamma_1}^q\big)(x) = f_q(x) = 0$, which is exactly the announced property.

Construction of Ψ: Let Π be the plane containing Γ_2, and d_2 its signed distance function, chosen positive in the interior of Γ_2 (note that at each point of Γ_2, d_2 is null). We consider the open set $\mathcal{O} = \Omega - \Pi$ and define function Ψ as the solution to the Cauchy problem defined on Ω:

$$\left\{ \begin{array}{ll} \nabla\Psi(p).\nabla U_{\Gamma_1}(p) = 0 & \text{if } p \in \mathcal{O}, \\ \Psi(p) = d_2(p) & \text{if } p \in \Pi, \\ \Psi(p) = \min(d_2) & \text{if } p \in \delta\Omega \end{array} \right. \tag{7}$$

where $\delta\Omega$ is the boundary of the image domain Ω. Problem (7) is known as a stationary transport problem and has been well studied in the modeling of geophysics phenomena.

Implementation: Unlike [12], minimal path are not to be computed. Using a Fast marching algorithm we compute U_{Γ_1} but no gradient descent is performed. In order to numerically solve problem (7), we use a simple iterative approach based on an *upwind* approximation of the gradients of Ψ and U_{Γ_1} [14]. More accurate approaches can be considered (see [15]) but, since we are only interested on the zero level set $\Psi^{-1}(0)$ this approach is sufficient. Lack of space forces us to skip the details.

4. APPLICATIONS

In this section we apply our method to a couple of 3D images. The first one, shown in figure 2, is a synthetic image obtained from three overlapping 'S' shaped closed tubes. Our method manages to extract the surface of the tube on which Γ_1 and Γ_2 are traced. The extraction of only one of these tubes is a difficult task for any variational segmentation approach since many local minima are present.
Our second example, shown in figure 3, is the extraction of the surface of the left ventricle from the 3D ultrasound image shown in figure 1.

5. CONCLUSION

In this paper we have presented a method that generalizes globally minimal paths to surfaces segmentation. Our model is initialized by two curves from which we take maximum advantage since the surface we generate is constrained to contain them. We have developed a novel implicit approach that, through a linear partial differential equation, exploits the solution to the eikonal equation and generates a function whose zero level set contains all the globally minimal paths between the constraining curves. Hence, our approach is not concerned by the problem of the local minima traps as all other active objects approach are. It is particularly well suited for medical image segmentation, in particular for ultrasound images segmentation. In cases where the image quality is very poor, our approach handles the introduction of additional information coming from the practitioner in a very natural manner. A few 2D segmentations can be enough to generate a coherent complete surface.

6. REFERENCES

[1] M. Kass, A. Witkin, and D. Terzopoulos, "Snakes: Active contour models," *International Journal of Computer Vision*, vol. 1, no. 4, pp. 321–331, 1988.

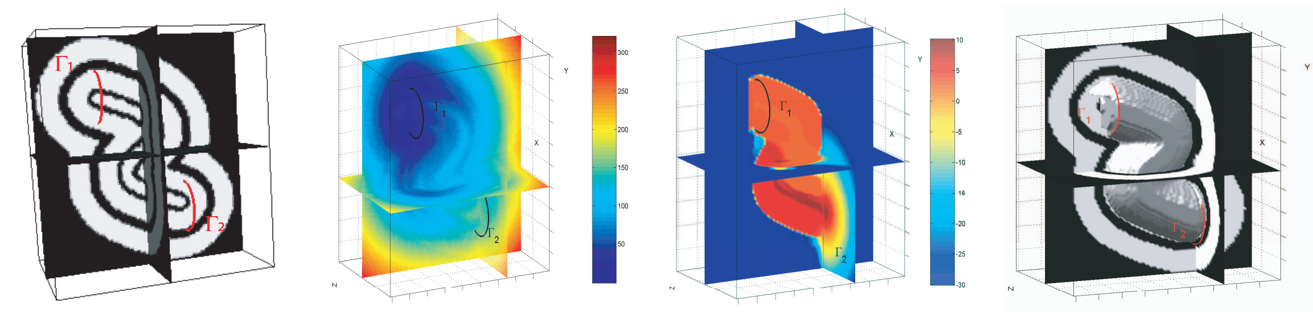

(a) (b) (c) (d)

Figure 2: Segmentation of a synthetic image : (a) shows three planes of the 3D image to segment and the position of Γ_1 and Γ_2. (b) shows the action map U_{Γ_1}. (c) shows the solution Ψ to the transport problem and (d) its zero level set. (see please the electronic color version).

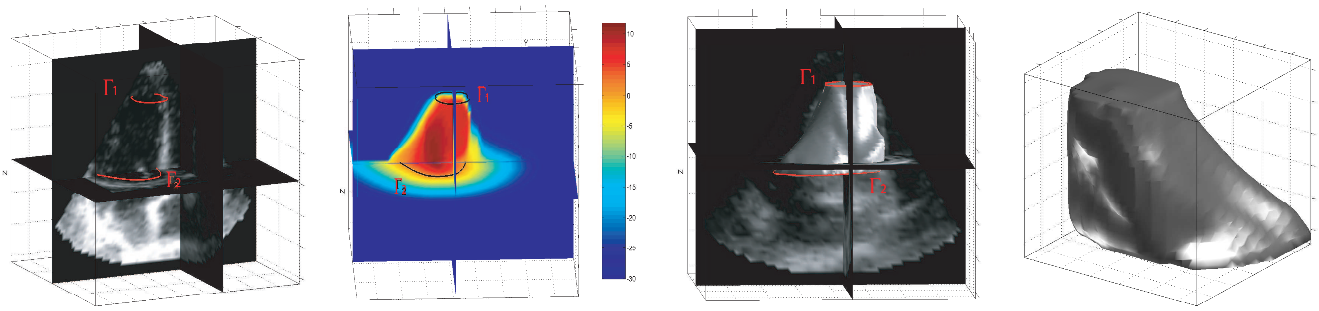

(a) (b) (c) (d)

Figure 3: Left ventricle segmentation : (a) shows three planes of the ultrasound image. (b) displays three planes of function Ψ obtained by our approach. (c) and (d) display the zero level set of Ψ, positioned in the image and zoomed. (see please the electronic color version).

[2] L.D. Cohen, "On active contour models and balloons," *CVGIP*, vol. 53, no. 2, pp. 211–218, 1991.

[3] Laurent Cohen, "Avoiding local minima for deformable curves in image analysis," in *Curves and Surfaces with Applications in CAGD*, Nashville, 1997, Vanderbilt Univ. Press.

[4] N. Paragios, *Geodesic Active Regions and Level Set Methods: Contributions and Applications in Artificial Vision*, Ph.D. thesis, Université Nice Sophia-Antipolis, 2000.

[5] A.L. Yuille, P.W. Hallinan, and D.S. Cohen, "Feature extraction from faces using deformable templates," *Int. J. of Computer Vision*, vol. 8, no. 2, pp. 99–111, August 1992.

[6] L.D. Cohen and R. Kimmel, "Global minimum for active contour models: A minimal path approach," *IJCV*, vol. 24, no. 1, pp. 57–78, Aug. 1997.

[7] V. Caselles, R. Kimmel, and G. Sapiro, "Geodesic active contours," *IJCV*, vol. 22, no. 1, pp. 61–79, 1997.

[8] A.M. Bruckstein, "On shape from shading," *CVGIP*, vol. 44, no. 2, pp. 139–154, November 1988.

[9] J. N. Tsitsiklis, "Efficient algorithms for globally optimal trajectories," *IEEE Transactions on Automatic Control*, vol. 40, no. 9, pp. 1528–1538, September 1995.

[10] J.A. Sethian, *Level set methods: Evolving Interfaces in Geometry, Fluid Mechanics, Computer Vision and Materials Sciences*, Cambridge University Press, 1999.

[11] T. Deschamps and L.D. Cohen, "Fast extraction of minimal paths in 3D images and applications to virtual endoscopy," *Medical Image Analysis*, vol. 5, no. 4, December 2001.

[12] R. Ardon and L.D. Cohen, "Fast Constrained Surface Extraction by Minimal Paths," *To appear in IJCV*, 2005.

[13] S. Osher and J.A. Sethian, "Fronts propagating with curvature dependent speed: algorithms based on the hamilton-jacobi formulation," *Journal of Computational Physics*, vol. 79, pp. 12–49, 1988.

[14] R. Ardon, L.D. Cohen, and A. Yezzi, "Implicit surface segmentation in 3D images by minimal paths," Tech. Rep., CEREMADE, 2005.

[15] Randall J. LeVeque, "High-resolution conservative algorithms for advection in incompressible flow," *SIAM J. Numerical Analysis*, vol. 33, no. 2, pp. 627–665, April 1996.